Simulation of blood flow and vessel deformation in three-dimensional, patient-specific models of the cardiovascular system using a novel method for fluid-solid interactions

A. Figueroa[1], I. Vignon-Clementel[1], K. Jansen[3], T. J. R. Hughes[4] & C. A. Taylor[1,2]
[1]*Department of Mechanical Engineering, Stanford University, USA*
[2]*Departments of Bioengineering and Surgery, Stanford University, USA*
[3]*Department of Mechanical, Aeronautical and Nuclear Engineering, Rensselaer Polytechnic Institute, USA*
[4]*Institute for Computational Engineering and Sciences (ICES), The University of Texas at Austin, USA*

Abstract

Blood velocity and pressure fields in large arteries are greatly influenced by the deformability of the vessel. However, computational methods for simulating blood flow in three-dimensional models of arteries have either considered a rigid wall assumption for the vessel or significantly simplified or reduced geometries. Computing blood flow in deformable domains using standard techniques like the ALE method remains a formidable problem for large, realistic anatomic and physiologic models of the cardiovascular system. We have developed a new method to simulate blood flow in three-dimensional deformable models of arteries. The method couples the equations of the deformation of the vessel wall at the variational level as a boundary condition for the fluid domain. We consider a strong coupling of the degrees-of-freedom of the fluid and the solid domains. The effect of the vessel wall boundary is therefore added in a monolithic way to the fluid equations, resulting in a remarkably robust scheme.
Keywords: finite element, three-dimensional, blood flow, wave propagation.



1 Introduction

In recent years, computational techniques applied to model blood flow in arteries have either examined only the velocity field (not the pressure field), treating the vessel walls of subject-specific models as rigid (e.g. Taylor *et al.*[1], Cebral *et al.*[2]), or have considered significantly simplified or reduced geometries of deformable wall models [3].

The rigid-wall approximation is made in large part because of the difficulty of solving the coupled blood flow / vessel deformation problem and is justified by the observation that, under normal conditions, wall deformability does not significantly alter the velocity field [3]. However, the assumption of rigid vessel walls precludes wave propagation phenomena, fundamentally changes the character of the resultant solutions, and results in difficulties in coupling three-dimensional domains with domains described using one-dimensional wave propagation methods [4].

One of the better-known methods for including wall deformability is the ALE (Arbitrarily Lagrangian - Eulerian) formulation for fluid-structure interaction problems [5]. However, ALE formulations are computationally expensive when considering large models of the vasculature. Application of fluid-structure interaction methods in simulation-based medical planning is additionally demanding in that multiple surgical interventions need to be modelled, solved, analyzed, and compared in a clinically relevant time-frame (hours). Simpler methods for incorporating wall motion are essential for these applications.

In this paper we present a new formulation for modelling blood flow in deformable arteries called the Coupled Momentum Method for Fluid-Solid Interaction problems (CMM-FSI). This formulation starts from a conventional stabilized finite element formulation for the Navier-Stokes equations in a rigid domain and modifies it in such a way that the deformability of the wall domain surrounding the fluid is taken into account. The main features of this formulation can be summarized as follows:

1. The *zero-velocity condition is removed* from the lateral surface of the fluid domain and replaced with a traction condition which is to be determined using the elastodynamics equations that describe the motion of the vessel wall.

2. Using a *thin wall approximation*, this unknown interface traction can be related to a body force for the vessel wall.

3. This *body force can be related through the elastodynamics equations* with the mass and stiffness terms of the vessel wall.

4. A *membrane formulation* is used to describe the mass and stiffness terms of the solid. The advantage of this approach is that no additional degrees-of-freedom beyond the membrane wall velocities are needed.

5. A *strong coupling* approach is used whereby the degrees-of-freedom of the vessel wall and the fluid boundary are the same. This results in a monolithic algorithm where the solid momentum contributions are embedded into the fluid equations using the same degrees-of-freedom.

6. A *linearized kinematics* approach is adopted for the coupled problem. This enables a representation of the solid equations using the same Eulerian frame as

in the fluid equations. Furthermore, the fluid mesh is kept fixed and therefore the computational time compared to ALE formulations is greatly reduced.
7. A linear membrane *enhanced with transverse shear modes* is used due to the inherent lack of stability of the linear membrane under transverse loading.

With this approach, the effects of the vessel wall motion are embedded in the weak form representing the blood flow resulting in a single weak form for the combined problem. As a result of this, only minimal changes in the stiffness matrices and residuals of the rigid wall finite element formulation are required to incorporate the effects of the wall motion. The approach delineated here results in a tractable, efficient and robust procedure to simulate fluid-structure interactions in three-dimensional models of the cardiovascular system. The computational effort is comparable to that of rigid wall formulations while at the same time it respects the essential physics and enables realistic simulation of wave-propagation phenomena in the arterial system as well as a linearized description of wall deformation.

2 Methods

2.1 Governing equations

2.1.1 Blood flow equations

Blood flow in large vessels of the cardiovascular system can be approximated as the flow of an incompressible Newtonian fluid in a domain Ω (see fig. 1). The weak form of the problem can be written as: find $\vec{v} \in \vec{\mathcal{S}}_h^k$ and $p \in \mathcal{P}_h^k$ such that

$$
\begin{aligned}
&B_G(\vec{w}, q; \vec{v}, p) = \\
&\int_\Omega \left\{ \vec{w} \cdot \left(\rho \vec{v}_{,t} + \rho \vec{v} \cdot \nabla \vec{v} - \vec{f} \right) + \nabla \vec{w} : \left(-p \underset{\sim}{I} + \underset{\sim}{\tau} \right) - \nabla q \cdot \vec{v} \right\} d\vec{x} \\
&+ \int_{\Gamma_h} \left\{ -\vec{w} \cdot \vec{h} + q v_n \right\} ds + \int_{\Gamma_s} \left\{ -\vec{w} \cdot \vec{t}^{\,f} + q v_n \right\} ds + \int_{\Gamma_g} q v_n ds = 0
\end{aligned}
\tag{1}
$$

for all $\vec{w} \in \vec{\mathcal{W}}_h^k$ and $q \in \mathcal{P}_h^k$. The functional spaces $\vec{\mathcal{S}}_h^k$, $\vec{\mathcal{W}}_h^k$ and $\mathcal{P}_h^k$ represent the equal-order interpolation spaces in $H^1(\Omega)$ for the velocity $\vec{v}$, the test function $\vec{w}$ and the pressure p as defined in [6].

Here, ρ is the blood density, $\vec{f}$ is the prescribed body force per unit volume and $\underset{\sim}{\tau}$ is the viscous stress tensor. Γ_g represents the fraction of the boundary where the given velocity field represented by $\vec{g}$ is prescribed. Γ_h and Γ_s represent Neumann boundaries where the tractions $\vec{h}$ and $\vec{t}^{\,f}$ are prescribed. Γ_h refers typically to an outflow boundary, and the traction $\vec{h}$ can be calculated using a constant traction, resistance or impedance boundary condition. The lateral boundary of the fluid domain is depicted by Γ_s. This part represents the interface with the vessel wall.

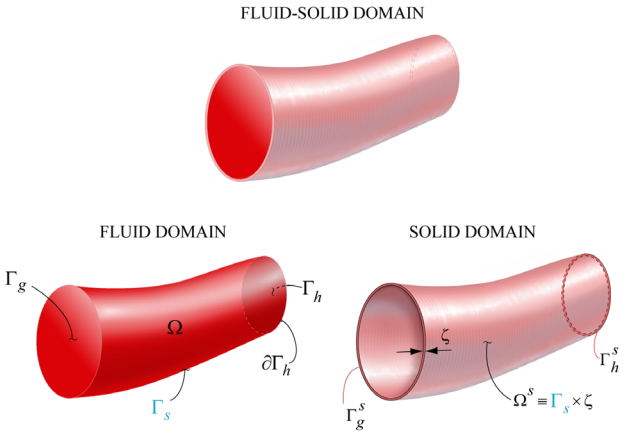


Figure 1: Schematic representation of the fluid and solid domains.

While a no-slip boundary condition would be prescribed on Γ_s in the case of a rigid wall approximation, this constraint is removed here to enable non-zero wall velocity and replaced by a traction $\bar{t}^f$. This traction is due to the interaction of blood and the vessel wall. At this point, this traction is unknown but it will be ultimately related with the stiffness and mass of the vessel wall using the elastodynamics equations of the solid. Before describing the treatment of the solid domain, it is important to recall that the standard Galerkin method is unstable for advection-dominated flows and in the diffusion dominated limit for equal-order interpolation of velocity and pressure. A stabilized method as described in [7] is utilized to address these deficiencies of Galerkin's method.

2.1.2 Vessel wall equations

The classic elastodynamics equations are used to describe the motion of the vessel wall in a domain Ω^s (see fig. 1). The vessel wall mechanics are herein approximated using a thin-walled structure assumption, and therefore the solid domain Ω^s can be topologically related to the lateral boundary of the fluid domain Γ_s. In fig. 1, Γ^s_g and Γ^s_h represent the parts of the boundary of Ω^s where the essential ($\bar{g}^s$) and natural ($\bar{h}^s$) boundary conditions are prescribed. In order to relate the elastodynamics equations with the lateral boundary of the fluid domain, Ω^s needs to be mapped on Γ_s. The solid's weak form defined in the domain Ω^s will be related to the fluid traction integral on the lateral boundary of the fluid domain

$$-\int_{\Gamma_s} \bar{w} \cdot \bar{t}^f \, ds \tag{2}$$

Assuming a thin-walled structure, integrals defined on Γ^s_h and Ω^s can be related with integrals on the lateral boundary of the fluid domain Γ_s according to the following expressions

$$\int_{\Omega^s}(\bullet)\,dx = \zeta\int_{\Gamma_s}(\bullet)\,ds \quad , \quad \int_{\Gamma_h^s}(\bullet)\,ds = \zeta\int_{\partial\Gamma_h}(\bullet)\,dl \tag{3}$$

where ζ represents the vessel wall thickness.

The surface traction $\vec{t}^{\,f}$ acting on the fluid lateral boundary due to the interaction with the solid is equal and opposite of the surface traction $\vec{t}^{\,s}$ acting on the vessel wall due to the fluid. Invoking again the thin wall approximation, this surface traction $\vec{t}^{\,s}$ can be related to a body force $\vec{b}^{\,s}$ acting on the solid domain since for a thin-enough structure the internal surface traction $\vec{t}^{\,s}$ will be felt uniformly through the wall thickness ζ. Therefore, it follows that

$$\vec{b}^{\,s} = -\vec{t}^{\,f}\Big/\zeta \tag{4}$$

and thus it is possible to relate the unknown integral term given by equation (2) with the weak form for the vessel wall problem. This approach to the coupling of the fluid and solid momentum equations is analogous to Womersley's [8] derivation of an analytical solution for axisymmetric pulsatile blood flow in a cylindrical elastic vessel. Considering the expression for the body force $\vec{b}^{\,s}$ given by eqn (4), the weak form for the solid domain can be written as follows:

$$-\int_{\Gamma_s}\vec{w}\cdot\vec{t}^{\,f}\,ds = \zeta\int_{\Gamma_s}\rho^s\vec{w}\cdot\vec{v}_{,t}\,ds + \zeta\int_{\Gamma_s}\nabla\vec{w}:\underset{\sim}{\sigma}^s\,ds - \zeta\int_{\partial\Gamma_h}\vec{w}\cdot\vec{h}^{\,s}\,dl \tag{5}$$

2.2 Combined formulation: the coupled momentum method for fluid-solid interaction

Equation (5) provides an expression for the unknown term in equation (1) as a function of the solid internal stresses and inertial forces. Combining these two equations results in the following weak Galerkin form for the CMM-FSI method:

$$\begin{aligned} &B_G(\vec{w},q;\vec{v},p) = \\ &\int_\Omega\left\{\vec{w}\cdot\left(\rho\vec{v}_{,t}+\rho\vec{v}\cdot\nabla\vec{v}-\vec{f}\right)+\nabla\vec{w}:\left(-p\underset{\sim}{I}+\underset{\sim}{\tau}\right)-\nabla q\cdot\vec{v}\right\}d\vec{x} \\ &-\int_{\Gamma_h}\vec{w}\cdot\vec{h}\,ds \;+\int_{\Gamma_h}qv_n\,ds \;+\int_{\Gamma_g}qv_n\,ds \\ &\boxed{+\zeta\int_{\Gamma_s}\left\{\vec{w}\cdot\rho^s\vec{v}_{,t}+\nabla\vec{w}:\underset{\sim}{\sigma}^s(\vec{u})\right\}ds-\zeta\int_{\partial\Gamma_h}\vec{w}\cdot\vec{h}^{\,s}\,dl+\int_{\Gamma_s}qv_n\,ds} \end{aligned} \tag{6}$$

2.3 Finite element model for the wall and time integration

In order to complete the formulation of the method, we need to discuss the details of the mechanical model for the vessel wall, in particular the characterization of the vessel wall stress tensor $\underset{\sim}{\sigma}^s(\vec{u})$. We are interested in

having a simple description of the wall mechanics in order to keep the computational cost of the method close to that of rigid wall theories. Furthermore, since we do not want to introduce additional degrees-of-freedom in the solid or re-mesh the fluid boundary mesh, a linear membrane element stabilized with through-plane shear represents a very convenient option.

The local stress and strain vectors for the vessel wall elements can be written as:

$$\begin{aligned}\left\{\bar{\sigma}^{s,l}\right\}^T &= \left[\sigma_{xx}^l,\quad \sigma_{yy}^l,\quad \tau_{xy}^l,\quad \tau_{xz}^l,\quad \tau_{yz}^l\right],\\ \left\{\bar{\varepsilon}^{l}\right\}^T &= \left[\frac{\partial u^l}{\partial x^l},\quad \frac{\partial v^l}{\partial y^l},\quad \frac{\partial u^l}{\partial y^l}+\frac{\partial v^l}{\partial x^l},\quad \frac{\partial w^l}{\partial x^l},\quad \frac{\partial w^l}{\partial y^l}\right]\end{aligned} \tag{7}$$

Here $u^l, v^l,$ and w^l are the three components of the displacement vector $\bar{u}^l$ and x^l, y^l are the local nodal coordinates. We now define the material stiffness tensor for a plane stress state of an incompressible, isotropic solid augmented by the transverse shear stresses τ_{xz}^l and τ_{yz}^l. This tensor can be written as follows:

$$\underset{\sim}{D} = \frac{E}{\left(1-\nu^2\right)}\begin{bmatrix} 1 & \nu & 0 & 0 & 0 \\ \nu & 1 & 0 & 0 & 0 \\ 0 & 0 & 0.5\left(1-\nu\right) & 0 & 0 \\ 0 & 0 & 0 & 0.5k\left(1-\nu\right) & 0 \\ 0 & 0 & 0 & 0 & 0.5k\left(1-\nu\right) \end{bmatrix} \tag{8}$$

where E and ν are the Young's modulus and Poisson ratio coefficients respectively, and the parameter k accounts for a parabolic variation of transverse shear stress through the membrane.

Once the weak form given by eqn. (6) is discretized, we integrate the field variables in time using a Generalized-α method for the velocity and a Backward Euler method for the pressure as proposed by Jansen *et al.* [9]. We have modified this method to account for the time integration of the displacement field. More specifically, we have used Newmark's formula to relate the displacement field on Γ_s with the velocity and acceleration.

3 Results

3.1 Subject-specific abdominal aortic aneurysm (AAA) model under rest conditions

In this problem we consider a subject-specific model of an abdominal aortic aneurysm, including the renal arteries feeding the kidneys, the celiac and superior mesenteric arteries feeding the viscera, and the iliac arteries, including the internal iliac arteries (see fig. 2). The geometry and volumetric flow rates

were obtained from magnetic resonance imaging data. The measured flow rate at the level of the diaphragm was specified on the inlet face of the model, mapped to a Womersley velocity profile.

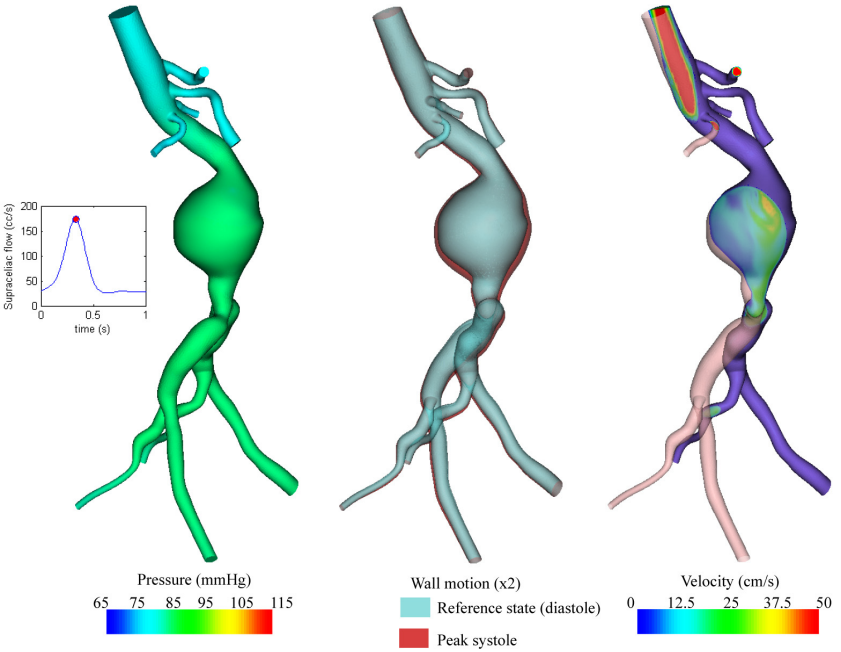


Figure 2: Pressure, wall displacement and blood velocity in a subject-specific AAA model under rest conditions. Blood pressure and velocity magnitude (along a slice plane) are shown at peak systole.

The cardiac cycle is T=1.05 s and the flow is Q=3.59 L/min. We utilized resistance boundary conditions for all eight outlet faces of the model based on the flow distribution acquired with MRI and completed with literature data [10] . The resistance values imposed at each of the eight outlet faces are shown in table 1. We have used a constant outlet pressure offset p_0 =72,870 dyn/cm^2 (55 mmHg) in order to obtain a physiologically realistic range of pressures in the solution. The Young's modulus of the vessel wall was prescribed to be $4.144 \cdot 10^6$ dynes/cm^2. Poisson's ratio is 0.5, the wall density 1.0 g/cm^3, the shear correction parameter is 5/6 and the mean wall thickness is 0.1 cm. The wall is fixed by constraining the degrees-of-freedom of the nodes located at the inlet and outlet rings. The solution was obtained using a 663,243 element and 135,522 node mesh with a time step of 0.4 ms, and 5 nonlinear iterations per time step, for a total of three cardiac cycles.

In this example, we observe that the pressure field shows a maximum value of 95 mmHg during peak systole. The velocity contour shows complex recirculating patterns with maximum velocities on the order of 50 cm/s at the

upper level of the abdominal aorta. The vessel wall deformation is moderate, consisting primarily in a radial expansion and contraction at the level of the aneurysm. These computations were performed with minimal increase (about a factor of two) in computational time compared to that of rigid wall theory.

Table 1: Resistances imposed at the outlet faces of the model during rest conditions.

	Celiac	SMA	Left renal	Right renal	Left iliac	Left int-iliac	Right Iliac	Right int-iliac
Resistance (dyn/cm^2)	1,946	2,622	2,622	2,622	2,912	6,790	2,912	6,790

3.2 Subject-specific abdominal aortic aneurysm (AAA) model under exercise conditions

In this problem we consider the same model as in the previous example but under simulated exercise conditions. The cardiac cycle is T=0.7 s and the flow is Q=10.77 L/min, this represents a three-fold increase. We have used a constant outlet pressure offset p_0 =68,726 dyn/cm^2 (51.2 mmHg) and the resistance values shown in table 2 in order to obtain a physiologically realistic range of pressures.

Table 2: Resistances imposed at the outlet faces of the model during exercise conditions.

	Celiac	SMA	Left renal	Right renal	Left iliac	Left int-iliac	Right Iliac	Right int-iliac
Resistance (dyn/cm^2)	2,694	3,630	3,630	3,630	823	1,918	823	1,918

The resistances imposed at the level of the iliacs show lower values than in the previous example to accommodate the much larger flow occurring in exercise conditions with a realistic increase in pressure.

Figure 3 shows the pressure, wall deformation and velocity contour along a slice plane at peak systole. We can observe that the pressure at the level of the aneurysm has increased by 20 mmHg. Similarly, the velocity field shows larger values throughout the model. But perhaps the most remarkable difference between this example and the previous one lies on the patterns of the wall deformation. In this case, the deformation of the wall is no longer occurring in a radial expansion and contraction fashion, but rather as a net motion forward and backwards due to the much larger inertial forces exerted on the wall by the impinging blood stream.

4 Conclusions

We have successfully developed and implemented a simple novel method for simulating blood flow in three-dimensional deformable models of arteries. We have applied the method to a clinically relevant problem, showing its potential to

represent blood flow and vessel wall deformation with computational costs comparable to those of rigid wall theories.

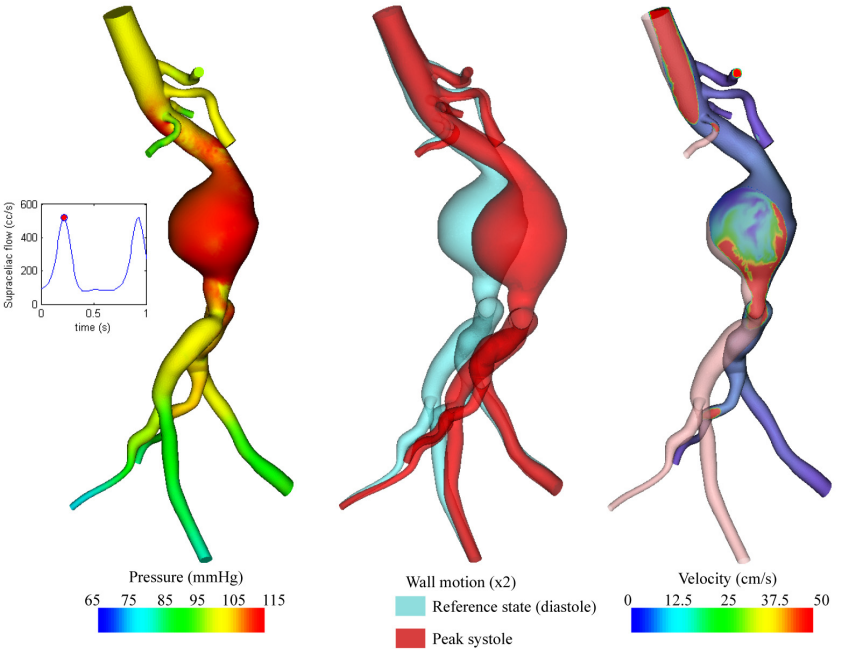


Figure 3: Pressure, wall displacement and blood velocity in a subject-specific AAA model under exercise conditions. Blood pressure and velocity magnitude (along a slice plane) are shown at peak systole.

Future improvements of the formulation will account for the effects of the surrounding tissue, vessel wall viscoelasticity and anisotropy. Furthermore, it is also possible to improve the behaviour of the enhanced membrane model of the vessel wall in regions of significant bending using rotation-free shell triangles.

Finally, the method should be validated against analytical solutions (i.e., Womersley's elastic solution) and *in vitro* and *in vivo* experiments.

Acknowledgement

This material is based upon work supported by the National Science Foundation under Grant No. 0205741.

References

[1] Taylor, C.A., Hughes, T.J.R. & Zarins, C.K. Finite Element modeling of blood flow in arteries. *Computer Methods in Applied Mechanics and Engineering*, **158**, pp. 155-196, 1998.

[2] Cebral, J.R., Castro, M.A., Soto, O., Lohner, R. & Alperin, N. Blood-flow models of the circle of Willis from magnetic resonance data. *Journal of Engineering Mathematics*, **47(3-4)**, pp. 369-386, 2003.

[3] Perktold, K. & Rappitsch, G. Computer simulation of local blood flow and vessel mechanics in a compliant carotid artery bifurcation model. *Journal of Biomechanics*, **28(7)**, 845-856, 1995.

[4] Formaggia, L., Gerbeau, J.F., Nobile, F. & Quarteroni, A. On the coupling of 3D and 1D Navier-Stokes equations for flow problems in compliant vessels. *Computer Methods in Applied Mechanics and Engineering*, **191(6/7)**, pp. 561-582, 2001.

[5] Hughes, T.J.R., Liu, W.K. & Zimmermann, T.K. Lagrangian-Eulerian Finite Element formulation for incompressible viscous flows. *Computer Methods in Applied Mechanics and Engineering*, **29**, pp. 329-349, 1981.

[6] Whiting, C.H. & Jansen, K.E. A stabilized Finite Element method for the incompressible Navier-Stokes equations using a hierarchical basis. *International Journal for Numerical Methods in Fluids*, **35**, pp. 93-116, 2001.

[7] Hughes, T.J.R., Franca, L.P. & Balestra, M. New Finite Element formulation for computational fluid dynamics: V. Circumventing the Babuska-Brezzi condition: A stable Petrov-Galerkin formulation of the Stokes problem accomodating equal-order interpolations. *Computer Methods in Applied Mechanics and Engineering*, **59(1)**, pp. 85-99, 1986.

[8] Womersley, J.R. Oscillatory motion of a viscous liquid in a thin walled elastic tube-I: The linear approximation for long waves. *The Philosophical Magazine*, **7**, pp. 199-221, 1955.

[9] Jansen, K.E., Whiting, C.H. & Hulbert, G.M. Generalized-alpha method for integrating the filtered Navier-Stokes equations with a stabilized Finite Element method. Computer Methods in Applied Mechanics and Engineering, **190(3-4)**, pp. 305-319, 2000.

[10] Guyton, A.C., M.D. *Physiology of the human body*. San Francisco, Saunders College Publishing, 1984.

